H/D isotope effects on NMR chemical shifts of nuclei involved in a hydrogen bridge of hydrogen isocyanide complexes with fluoride anion

Nikolai S. Golubev,[a] Carsten Detering,[b] Sergei N. Smirnov,[a] Ilja G. Shenderovich,[ab] Gleb S. Denisov,[a] Hans-Heinrich Limbach[b] and Peter M. Tolstoy*[ab]

Received 7th January 2009, Accepted 23rd February 2009
First published as an Advance Article on the web 3rd April 2009
DOI: 10.1039/b900152b

^{1}H, ^{2}H, ^{19}F and ^{15}N NMR spectra of a strongly hydrogen-bonded anionic cluster, $CNHF^{-}$, as an ion pair with a tetrabutylammonium cation dissolved in CDF_3–CDF_2Cl mixture were recorded in the slow exchange regime at temperatures down to 110 K. The fine structure due to spin–spin coupling of all nuclei involved in the hydrogen bridge was resolved. H/D isotope effects on the chemical shifts were measured. The results were compared with those obtained earlier for a similar anion, FHF^{-}, and interpreted *via ab initio* calculations of magnetic shielding as functions of internal vibrational coordinates, namely an anti-symmetric proton stretching and a doubly-degenerate bending. The values of primary and secondary isotope effects on NMR chemical shifts were estimated using a power expansion of the shielding surface as a function of vibrational coordinates. A positive primary isotope effect was explained as a result of the decrease of the hydron stretching amplitude upon deuteration. We show that the proton shielding surface has a minimum close to the equilibrium geometry of the $CNHF^{-}$ anion, leading to the positive primary H/D isotope effect in a rather asymmetric hydrogen bond. We conclude that caution should be used when making geometric estimations on the basis of NMR data, since the shapes of the shielding functions of the internal vibrational coordinates can be rather exclusive for each complex.

Introduction

H/D isotope effects on NMR chemical shifts of nuclei involved in a hydrogen bridge are often used in studies of hydrogen-bonded systems, providing valuable information on proton location inside the bridge. For example, a positive primary isotope effect, *i.e.* when the bridging deuteron is deshielded as compared to the proton, is usually considered as an indication of a single central (or nearly central) proton position inside the H-bond.[1–4] An interesting system of this type, a 1 : 1 complex of a HF molecule with collidine, which contains a hydrogen bond of type NHF, has been previously studied experimentally[5–7] and theoretically.[8] It has been shown that the sign of the primary isotope effect changes from negative to positive upon strengthening (shortening) of the hydrogen bond.[5] Another typical system exhibiting a positive primary H/D isotope effect, the centrosymmetric hydrogen difluoride anion (FHF^{-} as an ion pair with tetrabutylammonium cation, TBA^{+}) dissolved in a CDF_3–CDF_2Cl mixture, has also been investigated by low-temperature ^{1}H, ^{2}H and ^{19}F NMR spectroscopy.[9] It has been found that two chemically equivalent ^{19}F nuclei are shielded upon deuteration of the anion (negative secondary isotope effect), though a one-dimensional model predicts fluorine deshielding.[1] In ref. 10, the contributions of different normal vibrations to the H/D isotope effects on ^{1}H and ^{19}F chemical shifts for FHF^{-} have been analyzed. It has been demonstrated that the positive primary isotope effect originates mainly from the diminishing amplitude of the longitudinal (anti-symmetric) proton vibration, whereas the main cause of the negative secondary effect on ^{19}F is a decrease in the amplitude of the doubly-degenerate bending vibration. The symmetric stretching vibration contributes very slightly to the overall effect.[10]

In the present contribution we report the results of a study of a chemically similar system, $TBA^{+}CNHF^{-}$, that is, hydrogen fluoride isocyanide with tetrabutylammonium as a counter cation. The structure of the cluster as $CNHF^{-}$ rather than $NCHF^{-}$ will be proven in the Discussion section by considering the values of experimentally observed scalar couplings. The results are rationalized by means of *ab initio* computations of one-dimensional magnetic shielding surfaces as functions of internal coordinates characterizing proton position in the hydrogen bridge and compared with those obtained previously for FHF^{-}.

Experimental

Synthesis and sample preparation

The complex salt, $TBA^{+}C^{15}NHF^{-}$, was prepared by bubbling anhydrous gaseous $HC^{15}N$ into $TBA^{+}F^{-}$ dissolved in CD_2Cl_2 and cooled to 190 K. Prior to this, tetrabutylammonium fluoride was dried by repeated azeotropic distillation with CH_2Cl_2 under reduced pressure in a rotor evaporator.

[a] *V. A. Fock Institute of Physics, St. Petersburg State University, Uljanovskaja 1, 198504, St. Petersburg, Russia*
[b] *Institute of Chemistry and Biochemistry, Free University of Berlin, Takustr. 3, 14195, Berlin, Germany. E-mail: tolstoy@chemie.fu-berlin.de; Fax: +49 30 838 55310; Tel: +49 30 838 53615*

Hydrogen cyanide enriched with ^{15}N was prepared from $NaC^{15}N$ (Aldrich, 96% isotopic purity) and phosphoric acid and purified by repeated distillation under reduced pressure. $DC^{15}N$ was prepared analogously with phosphoric acid-d_3. The solvent, CDF_3–CDF_2Cl mixture which freezes below 100 K, was prepared according to the procedure described in ref. 11.

Several μL of the solution of the resulting salt, TBA hydrogen (deuterium) fluoride isocyanide, in CD_2Cl_2 were placed in a hermetic thick-walled NMR sample tube equipped with a PTFE valve (Wilmad), connected to a high vacuum line, and filled with the CDF_3–CDF_2Cl mixture *via* vacuum transfer. On performing this procedure, the exact total concentration of the salt remained unknown. A rough estimate gives a total concentration of about 0.03 mol L^{-1}.

NMR spectra

A Bruker AMX-500 NMR spectrometer equipped with a low-temperature probe which allowed us to perform experiments down to 100 K was used. ^1H, ^2H and ^{19}F NMR chemical shifts were measured using CHF_2Cl as internal standard and converted to the conventional scales (TMS for ^1H spectra, TMS-d_{12} for ^2H and $CFCl_3$ for ^{19}F). ^{15}N NMR chemical shifts were referenced to NH_4Cl as external standard. The total deuterium fraction x_D was determined by comparison of the integrated intensities of N(H) and N(D) peaks in the ^{15}N spectra measured without proton decoupling.

QM computations

The optimized geometry of the hydrogen bridge in an isolated $CNHF^-$ ion, harmonic force field and normal vibrational frequencies were calculated using Gaussian 98[12] at the MP2/6-311++G(3d, 3f) level of theory. Magnetic shielding functions were computed using the GIAO method, included in the same package, at the same level. The ground state expectation values of variables $r = r_{NH} - r_{HF}$, r^2 and φ^2 (deviation of the hydrogen bond from linearity) were evaluated *via* solving two anharmonic one-dimensional vibrational problems with potential functions on r and φ variables, obtained *ab initio* (for brevity, these potential functions are not presented in this paper).

Nomenclature

Throughout this paper chemical shifts are labeled as δ(NLF), where the observed nucleus is given in italics and L = H, D. A similar nomenclature is used for the coupling constants, such as $^{2h}J(NHF)$, and magnetic shieldings, such as $\sigma(NLF)$. From the differential line broadenings visible in the ^1H and ^{15}N NMR spectra presented below it is possible to establish that $^{2h}J(NHF)$, $^1J(NHF)$ and $^1J(NHF)$ coupling constants are negative,[7] however in this paper we omit the signs and discuss only the absolute values of the coupling constants.

Results

NMR spectra

The low field parts of the ^1H and ^2H NMR spectra of the salt TBA^+CNHF^- dissolved in a freon mixture, CDF_3–CDF_2Cl, are represented in Fig. 1. At 130 K, the ^1H spectrum is comparatively well resolved and consists of a doublet of doublets, due to spin–spin coupling with both ^{15}N and ^{19}F nuclei ($^1J(NHF)$ = 91.6 Hz, $^1J(NHF)$ = 63.4 Hz; assignment of the couplings will become apparent when ^{15}N and ^{19}F NMR spectra are considered). Upon deuteration the signal of the bridging hydron is shifted to low field: the primary H/D isotope effect is positive, $\delta(NDF) - \delta(NHF) = +0.15$ ppm. The linewidths in the ^2H NMR multiplet are larger than those in the ^1H NMR multiplet due to quadrupolar deuteron relaxation.

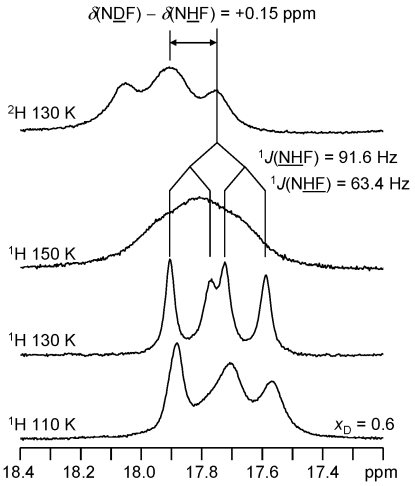

Fig. 1 ^1H and ^2H NMR spectra of TBA^+CNHF^- (TBA^+CNDF^-) (96% ^{15}N, x_D = 0.6) dissolved in CDF_3–CDF_2Cl measured at low-temperatures.

Line broadening in the ^1H NMR spectra at temperatures different from 130 K (see Fig. 1) can be explained as follows. Increasing the temperature above 130 K leads to accelerated chemical exchange processes; lowering the temperature below 130 K results in differential line broadening due to the fast dipolar and anisotropic mechanisms of spin relaxation (different spin states are characterized by different lifetimes).[9] Not only linewidths, but also the ^1H NMR chemical shift itself is temperature dependent. The direction of the temperature dependence—signal shifts to the high field upon cooling (see Fig. 1)—points to hydrogen bond weakening with decreasing temperature.

The ^{15}N NMR spectrum of the non-deuterated species, $CNHF^-$, measured at 130 K (Fig. 2, bottom) consists of a doublet of doublets with coupling constants $^1J(NHF)$ = 92 Hz, $^{2h}J(NHF)$ = 61 Hz. For the measurement of the H/D isotope effect on the nitrogen chemical shift, the maximal extent of deuteration attainable for the sample preparation procedure described in the Experimental section was used, x_D = 0.96. The spectrum of the $CNDF^-$ anion recorded for a deuterated sample is represented in the top part of Fig. 2. It is seen that H/D replacement results in a strong nitrogen shielding and the transformation of the doublet of doublets into a doublet of triplets. Spin–spin coupling constants $^{2h}J(NDF)$ and $^{2h}J(NHF)$ are the same within the precision of our measurements. The one-bond coupling constant $^1J(NDF)$ is equal to 14 Hz, thus $^1J(NHF)/^1J(NDF)$ is equal to 6.57 which coincides well with the ratio of the gyromagnetic ratios γ_{1H}/γ_{2H} = 6.51.

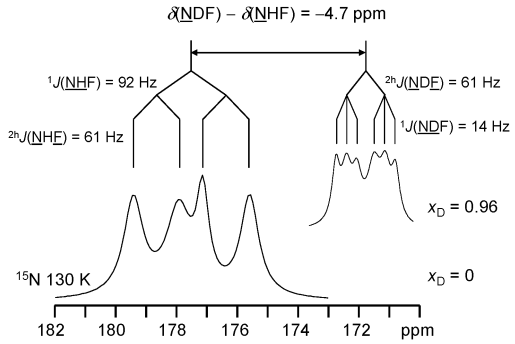

Fig. 2 ^{15}N NMR spectra of TBA^+CNHF^- (bottom, $x_D = 0$) and TBA^+CNDF^- (top, $x_D = 0.96$) dissolved in CDF_3–CDF_2Cl, measured at 130 K.

The linewidths of the *N*DF multiplet components are reduced as compared to those of the *N*HF multiplet because the efficiency of the dipolar ND relaxation is lower as compared to that of the NH one.

The ^{19}F NMR spectrum of TBA^+CNHF^- measured at 130 K is shown in Fig. 3. Since the values of ^1J(N*HF*) and ^{2h}J(*N*H*F*) coincide within the limits of the linewidth, the fluorine spectrum looks like a usual binomial triplet. The fluorine chemical shift of −152 ppm is very close to that reported previously for FHF^- (−155 ppm).[9] The H/D isotope effect on this value was not measured.

Ab initio calculations

The optimized geometry of the hydrogen bridge in the isolated $CNHF^-$ ion calculated at the MP2/6-311++G(3d,3f) level of theory is as follows: $r_{NH}^e = 1.09$ Å, $r_{HF}^e = 1.43$ Å, $r_{NF}^e = 2.52$ Å, $\alpha_{NHF} = 180°$. The asymmetry parameter $r^e = r_{NH}^e - r_{HF}^e = -0.34$ Å.

In Fig. 4 the calculated proton shielding σ(N*H*F) is plotted as the function of the asymmetry parameter $r = r_{NH} - r_{HF}$ for the $CNHF^-$ anion. The positions of all the heavy atoms were fixed during these calculations. The calculated shieldings are relative to the free CNH molecule. For comparison, on the same plot we show the shielding σ(F*H*F) calculated as the function of $r = r_{FH} - r_{HF}$ for the FHF^- anion (here, shieldings are relative to the free FH molecule; calculations were performed in the same way as for $CNHF^-$). In Fig. 5, similar plots are shown for the calculated heavy-atom shieldings σ(*N*HF) and σ(*F*H*F*). It is to be noted that on the NMR time scale the vibrational motion is always fast and

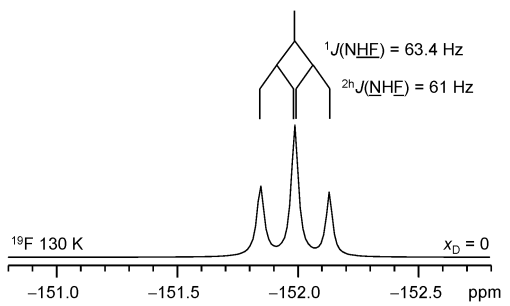

Fig. 3 ^{19}F NMR spectrum of TBA^+CNHF^- ($x_D = 0$) dissolved in CDF_3–CDF_2Cl, measured at 130 K.

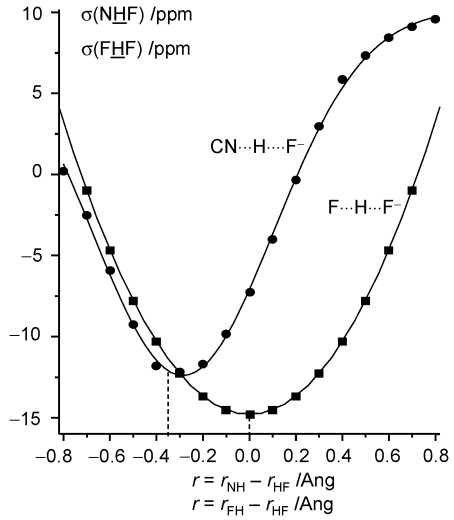

Fig. 4 The calculated (GIAO MP2/6-311++G(3d, 3f)) dependences of relative (with respect to free CNH and FH molecules) magnetic shielding of the protons in the $CNHF^-$ and FHF^- anions as functions of vibrational coordinate r. Equilibrium values of r are marked by dashed lines.

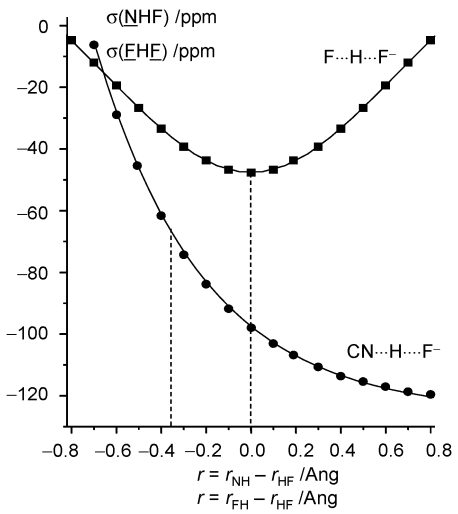

Fig. 5 The calculated (GIAO MP2/6-311++G(3d, 3f)) dependences of relative (with respect to free CNH and FH molecules) magnetic shielding of the ^{15}N and ^{19}F nuclei in the $CNHF^-$ and FHF^- anions as functions of vibrational coordinate r. Equilibrium values of r are marked by dashed lines.

for comparison with experiment the calculated nuclear shieldings of the two fluorine nuclei plotted in Fig. 5 are averaged, σ(*F*H*F*) = (σ(*F*HF) + σ(FH*F*))/2. Finally, dependences of the heavy-atom shieldings on the angle φ (deviation of the structure from the linear one, $\varphi = 180° - \alpha$) are shown in Fig. 6 for both anions. For the latter plot we set the magnetic shieldings of the linear structures to zero. Proton shielding dependence on the angle φ, symmetric with respect to $\varphi = 0$, has also been calculated for both anions but is not shown in this paper for brevity. The equilibrium values of the vibrational coordinates are marked by dashed lines in Fig. 4–6.

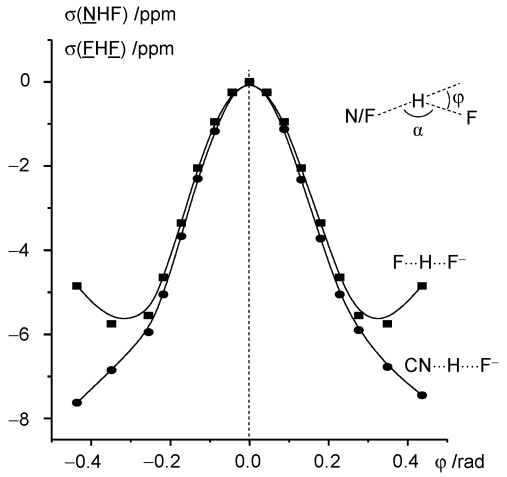

Fig. 6 The calculated (GIAO MP2/6-311 + + G(3d, 3f)) dependences of relative (with respect to linear configuration) magnetic shieldings of the ^{15}N and ^{19}F nuclei in the $CNHF^-$ and FHF^- anions as functions of vibrational coordinate φ. The equilibrium value of φ for both anions is marked by a dashed line.

Discussion

NMR spectra and the structure of the anion

The anionic cluster is formed as a result of the interaction of NCH with the fluoride anion involved in ion pairing with the TBA cation. The complexation is accompanied with tautomeric rearrangement, NCH → CNH. The driving force of this conversion is probably the formation of an $NH\cdots F^-$ hydrogen bond, which is apparently stronger than the $CH\cdots F^-$ one. The structure of the cluster as hydrogen isocyanide fluoride ($CNHF^-$) rather than hydrogen cyanide fluoride ($NCHF^-$) is proven by the value of the NH coupling constant $^1J(NHF)$ = 91.6 Hz (Fig. 1 and 2). Indeed, experimental values of $^2J(NCH)$ are in the range of 8–10 Hz[13] while scalar couplings of the type $^1J(HCNH^+)$ experimentally observed for protonated cyanides are in the range of 120–140 Hz.[14] These findings have also been supported by the QM calculations.[15,16] In the case of the $CNHF^-$ anion the reduction of the one-bond NH coupling down to 92 Hz is due to the formation of the strong hydrogen bond.

Two facts point out that the hydrogen bond in the $CNHF^-$ anion is a short one. Firstly, the ^{1}H chemical shift is 17.8 ppm (compared with the chemical shift of 16.4 ppm, measured for FHF^- under similar conditions).[9] Secondly, the primary isotope effect on the proton chemical shift is positive, $\delta(NDF) - \delta(NHF) = +0.15$ ppm, *i.e.* the deuteron is less shielded than the proton (the same is true for FHF^-, for which the primary isotope effect of +0.32 ppm has been measured).[9] We note that the positive primary isotope effect +0.27 ppm has been found previously for the HF complex with collidine, dissolved in a CDF_3–CDF_2Cl mixture at 145 K.[5] As mentioned in the introduction, this is usually considered as an indication of central or nearly central proton position inside the hydrogen bond. Moreover, for $CNHF^-$ a rather high value of the two-bond spin–spin coupling constant, $^{2h}J(NHF)$ = 61 Hz, indicates the covalent character of the hydrogen bond.[17] The reduced coupling constant $^{2h}K(NHF) = {}^{2h}J(NHF)/(\gamma_N\gamma_F)$ appears to be significantly higher than that for FHF^- ($^{2h}K(NHF)/{}^{2h}K(FHF)$ = 2.2;[18] bearing in mind that the $^{2h}J(FHF)$ and thus $^{2h}K(FHF)$ values cannot be measured but only calculated), though the F···F distance (2.299 Å according to ref. 9) is significantly shorter than the N···F distance, which is about 2.52 Å as our *ab initio* calculations show. This can be a result of a more pronounced s-character of the N atom in the $CNHF^-$ anion (~sp as compared to sp^3 hybridization of fluoride in FHF^-). We note that the $^{2h}K(NHN)$ reduced couplings calculated for the equilibrium structures of a number of $(RCNHNCR)^+$ complexes[16,19] are generally larger than the $^{2h}K(NHF)$ reported here. Values of $^{2h}J(RCNHNCR)$ are in the range of 20–40 Hz.

Using the example of a hydrogen-bonded complex formed by HF molecule with collidine, in ref. 7 it has been shown that chemical shifts and coupling constants can be used to estimate the interatomic distances within the NHF hydrogen bridge. From the experimentally found NMR parameters reported here and the correlation curves published in ref. 7 one can find the following geometric parameters for the $CNHF^-$ anion: r_{NH} = 1.07 Å, r_{HF} = 1.48 Å and r_{NF} = 2.55 Å. This compares well with the distances calculated *ab initio*: r_{NH}^e = 1.09 Å, r_{HF}^e = 1.43 Å, r_{NF}^e = 2.52 Å. Note that the estimated value of r_{NF} is larger than the equilibrium distance, r_{NF}^e. Most probably this is due to zero-point motions.

The calculation of Mulliken atomic charges, C(−0.23) N(+0.11) H(+0.12) F(−0.83), points to charge distribution along the chain, intermediate between three limiting structures, $C^-\equiv N^+–H\cdots F^- \leftrightarrow C{=}N–H\cdots F^- \leftrightarrow C^-\equiv N\cdots H–F$. However, the temperature dependence of the ^{1}H NMR spectra is characteristic for ion pairs of the type $NH^+\cdots F^-$[20] and can point to the domination of the bipolar limiting structure $C^-\equiv N^+–H\cdots F^-$ in the real charge distribution.

Magnetic shielding functions

From Fig. 4 it is apparent that the proton shielding functions for $CNHF^-$ and FHF^- have minima at approximately the equilibrium geometry of the corresponding anion. According to ref. 9, for FHF^- the main reason for this is paramagnetic deshielding caused by the hydrogen bond, which is maximal at the central proton position. For $CNHF^-$, the minimum is shifted towards the nitrogen atom due to, probably, a strong paramagnetic influence of the CN group itself. Previously it has been shown that for the strong NHF hydrogen bond in the collidine–HF 1 : 1 complex the maximal deshielding of the bridging proton is reached when $r = r_{NH} - r_{HF} = -0.1$ Å.[7,21] Thus, coincidence between the positions of the minima in the proton shielding and the potential surfaces for $CHNF^-$ at $r^e = -0.34$ Å is not likely to be explained simply by the fact that the heavy atoms of the H-bond are different.

The shapes of the ^{15}N (in $CNHF^-$) and ^{19}F (in FHF^-) shielding functions (Fig. 5) are qualitatively different. Namely, nitrogen shielding falls monotonously with proton approaching fluorine, while the fluorine shielding passes through a minimum at the equilibrium geometry of FHF^-. The main reason for this difference is the paramagnetic

contribution, which is very strong for the diatomic CN^- ion and equal to zero for the spherical F^- one.

The angle dependences of the ^{15}N and ^{19}F shieldings are practically identical near the equilibrium point $\varphi = 0$. The reason for nitrogen deshielding with increasing angle is probably as follows: every deviation from linearity increases the contribution of the limiting structure C=N–H···F^- with a double C=N bond instead of the triple one, as in $C^- \equiv N^+$–H···F^- and $C^- \equiv N$···H–F. The origin of the similar behavior of the fluorine shielding is not clear.

Calculation of the H/D isotope effects

A simplified method of calculation of H/D isotope effects on NMR chemical shifts has been described in ref. 10 and based on the general procedure explained in ref. 22 and 23. According to this method, if one takes into account only two normal vibrations most sensitive to H/D substitution, namely, the proton longitudinal stretching (coordinate r) and degenerate transverse bending (coordinate φ), the power expansion of the primary H/D isotope effect for the $CNHF^-$ anion can be written as in eqn (1):

$$\delta(\mathrm{N}D\mathrm{F}) - \delta(\mathrm{N}H\mathrm{F}) = -\left(\frac{\partial\sigma(\mathrm{N}H\mathrm{F})}{\partial r}\right)_e \Delta\langle r\rangle_0 - \frac{1}{2}\left(\frac{\partial^2\sigma(\mathrm{N}H\mathrm{F})}{\partial r^2}\right)_e \Delta\langle r^2\rangle_0 - \left(\frac{\partial^2\sigma(\mathrm{N}H\mathrm{F})}{\partial \varphi^2}\right)_e \Delta\langle \varphi^2\rangle_0 - \ldots, \quad (1)$$

where δ(NDF) and δ(NHF) are the deuteron and proton chemical shifts, σ(NHF) is the chemical shielding surface (identical for H and D isotopologs) and $\Delta\langle r\rangle_0$, $\Delta\langle r^2\rangle_0$ and $\Delta\langle \varphi^2\rangle_0$ are changes of the expectation values of the corresponding coordinates upon H/D substitution. Negative signs appear in the right hand-side of the expression due to the opposite directions of the chemical shielding and chemical shift scales. A linear term with respect to $\langle\varphi\rangle$ vanishes, as the equilibrium geometries of $CNHF^-$ and $CNDF^-$ are linear. The contribution of the symmetric stretching vibration is neglected in eqn (1) because according to ref. 10 it contributes very slightly to the overall effect. An expression similar to eqn (1) is valid also for the H/D isotope effect on ^{15}N NMR chemical shift, as in eqn (2):

$$\delta(N\mathrm{DF}) - \delta(N\mathrm{HF}) = -\left(\frac{\partial\sigma(N\mathrm{HF})}{\partial r}\right)_e \Delta\langle r\rangle_0 - \frac{1}{2}\left(\frac{\partial^2\sigma(N\mathrm{HF})}{\partial r^2}\right)_e \Delta\langle r^2\rangle_0 - \left(\frac{\partial^2\sigma(N\mathrm{HF})}{\partial \varphi^2}\right)_e \Delta\langle \varphi^2\rangle_0 - \ldots, \quad (2)$$

Note that in eqn (1) and (2) derivatives are taken at the equilibrium geometries, whereas the expectation values refer to the ground state. Since the geometries of these two states differ, such approximation increases possible errors. Thus, applying this method for our system we aim to find a qualitative rationalization of the observed H/D isotope effects, rather than to establish a quantitative agreement between the theoretical and experimental data.

The first and the second magnetic shielding derivatives were obtained numerically at the equilibrium geometries of $CNHF^-$ and FHF^- species using the dependences shown in Fig. 4–6. The resulting values are listed in Table 1 for $CNHF^-$ and in Table 2 for FHF^-. After multiplication of these derivatives by the changes of the expectation values upon deuteration (evaluated as described in the Experimental section) we have obtained contributions of individual vibrations into the overall isotope effects, which appeared to be quite close to the experimentally measured values. For example, for the $CNHF^-$ anion, the calculated value of the primary isotope effect is +0.19 ppm, while the experimental value is +0.15 ppm. Calculated and experimental secondary isotope effects are −3.31 ppm and −4.70 ppm, respectively.

The calculation of NMR isotope effects permits us to come to the following conclusions:

1. The approximation used reproduces correctly the signs and order of magnitude of the experimental values of the primary and secondary H/D isotope effects on the chemical shifts, despite simplifications of the model. The main reason for the deviations in the absolute values is, most probably, neglected normal vibrations of $CNHF^-$ which include motion of the heavy atoms. Another source of errors could be the neglected non-adiabatic paramagnetic mechanism of NMR isotope effects.

2. The position of the minimum on the σ(NHF) surface nearly coincides (presumably, by chance) with the equilibrium configuration of the anion. This diminishes the linear term in eqn (1) compared with the quadratic one and the latter determines the positive sign of the primary H/D isotope effect.

3. The signs of the secondary isotope effect on heavy nuclei for the two ions are identical. The absolute values differ by one order of magnitude. The dominant term for the isotope effect on the ^{15}N chemical shift in $CNHF^-$ is linear (see eqn (2)), and arises from an anharmonic NL bond contraction upon deuteration (L = H, D). In contrast to this, the dominant term for the isotope effect on ^{19}F in FHF^- is quadratic with respect to the angle variable φ. The corresponding term for $CNHF^-$ is even bigger, but small as compared to the linear one.

Conclusions

We conclude that the geometric estimations made on the basis of NMR data should be taken with caution, since the shapes of the shielding functions of the internal vibrational coordinates can be rather exclusive for each complex. For example, it has been previously shown for the FHF^- anion that the positive primary H/D isotope effect reflects mainly the decrease in the amplitude of the anti-symmetric stretching vibration upon deuteration (so called quadratic term), indicating the centrosymmetric position of the hydron.[10] For the non-symmetric $CNHF^-$ anion, studied in this paper, one could expect that the term associated with the NL bond contraction upon deuteration (linear term; L = H, D) would dominate and thus lead to the negative primary H/D isotope effect, typical for moderately strong hydrogen bonds. However, we show here that the proton shielding surface has a minimum close to the equilibrium geometry of the $CNHF^-$ anion and thus the linear term diminishes, leading to the positive primary H/D isotope effect in a rather asymmetric hydrogen bond.

Table 1 Derivatives of the shielding functions and changes of the expectation values of $r = r_{NH} - r_{HF}$, r^2 and φ^2 upon H/D substitution for $CNHF^-$. Isotope effects (IE) are calculated using eqn (1) and (2). For details see the text

		$\Delta\langle r\rangle_0$/Å	$\Delta\langle r^2\rangle_0$/Å^2	$\Delta\langle \varphi^2\rangle_0$/rad^2	Contribution to the IE (ppm)
$(\partial\sigma(\mathrm{NHF})/\partial r)$/ppm Å^{-1}	−7.7	−0.0106	—	—	−0.0820
$(\partial^2\sigma(\mathrm{NHF})/\partial r^2)$/ppm Å^{-2}	81.3	—	−0.0063	—	0.256
$(\partial^2\sigma(\mathrm{NHF})/\partial \varphi^2)$/ppm rad^{-2}	2.16	—	—	−0.0074	0.016
Overall IE[a] (ppm)	—	—	—	—	**+0.19 [+0.15]**
$(\partial\sigma(\mathrm{NHF})/\partial r)$/ppm Å^{-1}	−204.0	−0.0106	—	—	−2.162
$(\partial^2\sigma(\mathrm{NHF})/\partial r^2)$/ppm Å^{-2}	64.5	—	−0.0063	—	0.203
$(\partial^2\sigma(\mathrm{NHF})/\partial \varphi^2)$/ppm rad^{-2}	−183.0	—	—	−0.0074	−1.354
Overall IE[a] (ppm)	—	—	—	—	**−3.31 [−4.70]**

[a] In square brackets: experimental values.

Table 2 Derivatives of the shielding functions and changes of the expectation values of $r = r_{FH} - r_{HF}$, r^2 and φ^2 upon H/D substitution for FHF^-.[10] Isotope effects (IE) are calculated using eqn (1) and (2). For details see the text

		$\Delta\langle r\rangle_0$/Å	$\Delta\langle r^2\rangle_0$/Å^2	$\Delta\langle \varphi^2\rangle_0$/rad^2	Contribution to the IE (ppm)
$(\partial\sigma(\mathrm{FHF})/\partial r)$/ppm Å^{-1}	0	0	—	—	0
$(\partial^2\sigma(\mathrm{FHF})/\partial r^2)$/ppm Å^{-2}	76.5	—	−0.0078	—	0.298
$(\partial^2\sigma(\mathrm{FHF})/\partial \varphi^2)$/ppm rad^{-2}	2.07	—	—	−0.0058	0.012
Overall IE[a] (ppm)	—	—	—	—	**+0.31 [+0.32]**
$(\partial\sigma(\mathrm{FHF})/\partial r)$/ppm Å^{-1}	0	0	—	—	0
$(\partial^2\sigma(\mathrm{FHF})/\partial r^2)$/ppm Å^{-2}	98.2	—	−0.0078	—	0.383
$(\partial^2\sigma(\mathrm{FHF})/\partial \varphi^2)$/ppm rad^{-2}	−144.0	—	—	−0.0058	−0.835
Overall IE[a] (ppm)	—	—	—	—	**−0.45 [−0.37]**

[a] In square brackets: experimental values.

Acknowledgements

This work is supported by the Russian Foundation for Basic Research (grant no. 08–03-00615).

References

1 L. J. Altman, D. Laungani, G. Gunnarsson, H. Wennerström and S. Forsen, *J. Am. Chem. Soc.*, 1978, **100**, 8264; G. Gunnarsson, H. Wennerström, W. Egan and S. Forsen, *Chem. Phys. Lett.*, 1976, **38**, 96.

2 C. L. Perrin and J. B. Nielson, *J. Am. Chem. Soc.*, 1997, **119**, 12734.

3 P. Schah-Mohammedi, I. G. Shenderovich, C. Detering, H.-H. Limbach, P. M. Tolstoy, S. N. Smirnov, G. S. Denisov and N. S. Golubev, *J. Am. Chem. Soc.*, 2000, **122**, 12878.

4 H. H. Limbach, G. S. Denisov and N. S. Golubev, in *Isotope Effects In Chemistry and Biology*, ed. A. Kohen and H.-H. Limbach, Taylor & Francis, Boca Raton, FL, 2005, chapter 7, pp. 193–230.

5 I. G. Shenderovich, A. P. Burtsev, G. S. Denisov, N. S. Golubev and H.-H. Limbach, *Magn. Reson. Chem.*, 2001, **39**, S91.

6 N. S. Golubev, I. G. Shenderovich, S. N. Smirnov, G. S. Denisov and H. H. Limbach, *Chem.–Eur. J.*, 1999, **5**, 492.

7 I. G. Shenderovich, P. M. Tolstoy, N. S. Golubev, S. N. Smirnov, G. S. Denisov and H. H. Limbach, *J. Am. Chem. Soc.*, 2003, **125**, 11710.

8 J. E. Del Bene, R. J. Bartlett and J. Elguero, *Magn. Reson. Chem.*, 2002, **40**, 767.

9 I. G. Shenderovich, S. N. Smirnov, G. S. Denisov, V. A. Gindin, N. S. Golubev, A. Dunger, R. Reibke, S. Kirpekar, O. L. Malkina and H.-H. Limbach, *Ber. Bunsen-Ges. Phys. Chem.*, 1998, **102**, 422.

10 N. S Golubev, S. M. Melikova, D. N. Shchepkin, I. G. Shenderovich, P. M. Tolstoy and G. S. Denisov, *Z. Phys. Chem.*, 2003, **217**, 1549.

11 S. N. Smirnov, N. S. Golubev, G. S. Denisov, H. Benedict, P. Schah-Mohammedi and H.-H. Limbach, *J. Am. Chem. Soc.*, 1996, **118**, 4094.

12 M. J. Frisch, G. W. Trucks, H. B. Schlegel, G. E. Scuseria, M. A. Robb, J. R. Cheeseman, V. G. Zakrzewski, J. A. Montgomery,s Jr., R. E. Stratmann, J. C. Burant, S. Dapprich, J. M. Millam, A. D. Daniels, K. N. Kudin, M. C. Strain, O. Farkas, J. Tomasi, V. Barone, M. Cossi, R. Cammi, B. Mennucci, C. Pomelli, C. Adamo, S. Clifford, J. Ochterski, G. A. Petersson, P. Y. Ayala, Q. Cui, K. Morokuma, D. K. Malick, A. D. Rabuck, K. Raghavachari, J. B. Foresman, J. Cioslowski, J. V. Ortiz, B. B. Stefanov, G. Liu, A. Liashenko, P. Piskorz, I. Komaromi, R. Gomperts, R. L. Martin, D. J. Fox, T. Keith, M. A. Al-Laham, C. Y. Peng, A. Nanayakkara, C. Gonzalez, M. Challacombe, P. M. W. Gill, B. G. Johnson, W. Chen, M. W. Wong, J. L. Andres, M. Head-Gordon, E. S. Replogle and J. A. Pople, *Gaussian 98*, Gaussian, Inc., Pittsburgh, PA, 1998.

13 G. Binsch and J. D. Roberts, *J. Phys. Chem.*, 1968, **72**, 4310.

14 G. A. Olah and T. E. Kiovsky, *J. Am. Chem. Soc.*, 1968, **90**, 4666.

15 P. F. Provasi, G. A. Aucar, M. Sanchez, I. Alkorta, J. Elguero and S. P. A. Sauer, *J. Phys. Chem. A*, 2005, **109**, 6555.

16 H. Benedict, I. G. Shenderovich, O. L. Malkina, V. G. Malkin, G. S. Denisov, N. S. Golubev and H. H. Limbach, *J. Am. Chem. Soc.*, 2000, **122**, 1979.

17 I. Alkorta, J. Elguero and G. S. Denisov, *Magn. Reson. Chem.*, 2008, **46**, 599.

18 J. E. Del Bene, M. J. T. Jordan, S. A. Perera and R. J. Bartlett, *J. Phys. Chem. A*, 2001, **105**, 8399.

19 J. E. Del Bene and J. Elguero, *J. Phys. Chem. A*, 2006, **110**, 7496.

20 N. S. Golubev, G. S. Denisov, S. N. Smirnov, D. N. Shchepkin and H.-H. Limbach, *Z. Phys. Chem.*, 1996, **196**, 73.

21 I. G. Shenderovich, *Russ. J. Gen. Chem.*, 2006, **76**, 501.

22 A. D. Buckingham and R. M. Olegario, *Mol. Phys.*, 1997, **92**, 773.

23 R. D. Wigglesworth, W. Raynes, S. Kirpekar, J. Oddershede and S. Sauer, *J. Chem. Phys.*, 2000, **112**, 736.